

Imaging the charge transport in arrays of CdSe nanocrystals

M. Drndić,^{a)} R. Markov, M. V. Jarosz, M. G. Bawendi, and M. A. Kastner
Center for Material Science and Engineering, MIT, Cambridge, Massachusetts 02139

N. Markovic and M. Tinkham
Department of Physics, Harvard University, Cambridge, Massachusetts 02138

(Received 28 May 2003; accepted 18 September 2003)

A method to image charge is used to measure the diffusion coefficient of electrons in films of CdSe nanocrystals at room temperature. This method makes possible the study of charge transport in films exhibiting extremely high resistances or very small diffusion coefficients. © 2003 American Institute of Physics. [DOI: 10.1063/1.1626268]

Electric-force microscopy (EFM)¹ has been used to probe the electrical properties of microscopic systems, such as DNA molecules,² carbon nanotubes,³ SiGe dots,⁴ and single nanocrystals (NCs).⁵ However, there are few examples in which EFM data are analyzed quantitatively.⁵

We describe a method, based on EFM,¹ to image the charge motion in a regime not accessible to traditional transport measurements. We use it to directly obtain the charge diffusion coefficient in films of CdSe NCs. Semiconducting NC arrays made to date are so resistive that it is difficult to study them. The current through such arrays after application of a voltage step decays with time,^{6,7} so that the steady-state current corresponds to a resistance that is too large to measure by conventional means. Our technique could have wide application in highly resistive thin films.

The charge transport is imaged in three-dimensional arrays of CdSe NCs using a field-effect-transistor geometry.⁶ The EFM measurements are made after the voltage on the source electrode is turned on and off. The device, illustrated in Fig. 1, consists of two Au electrodes separated by $\sim 5 \mu\text{m}$, a 350-nm-thick SiO₂ layer, and the degenerately doped Si substrate. Highly monodispersed NCs, capped with trioctylphosphine oxide with $\approx 1.1 \text{ nm}$ between nearest neighbors,⁸ are self-assembled into $\sim 0.2\text{-}\mu\text{m}$ -thick films on top of the devices.⁶ We show data for two samples, with NC diameters 6.1 nm (Fig. 2) and 4.7 nm (Fig. 4). These NCs are synthesized using different preparations, as described in Refs. 8 and 9. Negative dc voltage V_{dc} is applied to the source electrode to charge the NCs, while all other voltages are zero (Fig. 1). Our approach is different from the standard EFM technique in which an ac voltage is applied to the tip.¹

We first discuss how the EFM provides a measure of the charge distribution. A small conductive tip oscillates in the z direction and is scanned parallel to the sample surface (Fig. 1). The electrostatic force F between the sample and the tip modifies its resonant frequency and introduces a phase shift $\Delta\phi(x,y) \propto dF/dz$.¹ An image is produced by measuring the phase shift as a function of the tip position in the xy plane at a constant height. The electrostatic force on the tip results from the capacitive coupling between the tip and the electrodes (or the gate) and from the Coulomb interaction between the static charges on the sample and the charges in-

duced on the tip and the electrodes (or the gate). Krauss *et al.*⁵ have discussed the force from a point charge. We use a similar argument before extending it to a charge distribution in the film. The charge q induces q_1 on the gate and q_2 on the tip. Following Ref. 5, $q_1, q_2 \propto q$, and ignoring contact potentials because we work with large voltages, and consequently, large charges q , one can show that $F \propto q^2$ for $V_{\text{dc}}=0$. The EFM signal is then $\Delta\phi \propto q^2$, proportional to the square of the charge.

We argue that the EFM signal for a continuous charge distribution is similarly proportional to the square of the charge in a small area of the film below the tip. We scan the tip $\sim 400 \text{ nm}$ above the film-SiO₂ interface, where the charge density resides. The strong electric field from the image charges in the Si substrate attracts the electrons toward the film-SiO₂ interface. Because this field is strong enough, we expect that only a few layers of NCs are populated. Because the oxide is $\sim 350 \text{ nm}$ thick, the image charge density in the gate is $\sim 350 \text{ nm}$ below that in the film. Thus, at lateral distances larger than $\sim 400 \text{ nm}$, the charge density in the film will be equal and opposite to the image charge in the Si substrate, giving a very small net force on the tip. The tip is only sensitive to charge within a radius of $\sim 400 \text{ nm}$. Considering only charges q, q_1 , and q_2 within this radius, this argument applies, and the force is once again proportional to q^2 .

We use a Digital Instruments atomic-force microscope with conducting tips. The tip scans twice over each line along x in the xy plane above the sample. In the first pass,

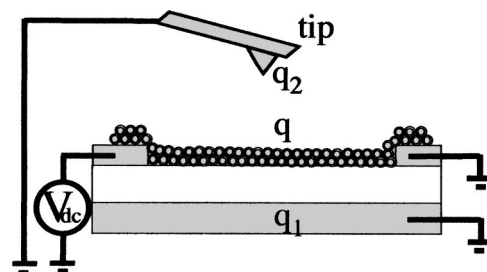


FIG. 1. Schematic diagram of the device and the EFM measurement setup. CdSe NCs are deposited on top of a device. For voltage $V_{\text{dc}} < 0$ on the source electrode electrons are injected into the film from the source; no charge injection is observed for positive voltages on the source. q is the charge on the sample, while q_1 and q_2 are charges induced by q in the gate and in the tip, respectively.

^{a)}Electronic mail: drndic@physics.upenn.edu

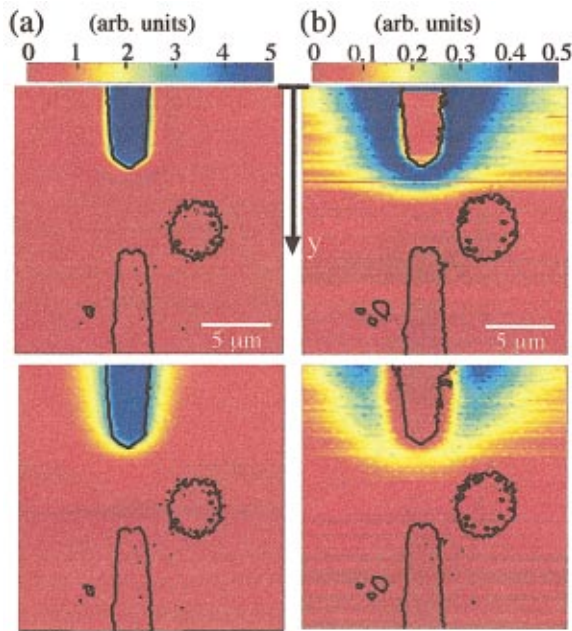


FIG. 2. (Color) (a) Charging and (b) discharging of a CdSe film as a function of time. A topographic contour containing the two electrodes is shown. The circle to the right of the electrodes is a flaw in the NC film.

the tip traces the topography by scanning close to the surface.¹ In the second pass above the same line, the tip is raised to a larger height (200 nm). Using the topographic profile, the tip is maintained at a constant height while the EFM signal is recorded. Each scan takes ≈ 3 min. At the end of each scan, the tip is moved back to the top of the image before the next scan. Because of significant spatial drifts over long time periods, we scan the topography of every line before each EFM scan. Samples are measured in a nitrogen gas atmosphere to prevent degradation.

Figure 2(a) shows the time evolution of EFM images with $V_{dc} = -40$ V applied to the source electrode. The topographical contour of the same region containing the electrodes is superimposed. V_{dc} is changed from 0 to -40 V at the top of the first scan, and it is held constant during the following scans. The second image is recorded 39 min after

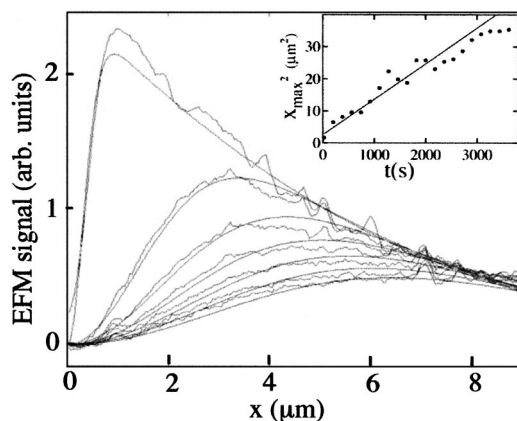


FIG. 3. The measured and calculated EFM signal plotted along the x axis during the discharging of the film. The calculated curves $[Q(x, t_j)]^2$ are obtained from the best fit of a diffusion model. The diffusion coefficient from the fit is $D = (2.8 \pm 0.2) \times 10^{-3} \mu\text{m}^2/\text{s}$. The comparison between data and theory shown for $t_j, j = 1, 4, \dots, 19$. Inset: Positions of maxima $x_{\text{max},j}$ vs time $t_j, j = 1$ to 21, and a linear fit $x_{\text{max}}^2 = 4Dt$, giving the same value of D .

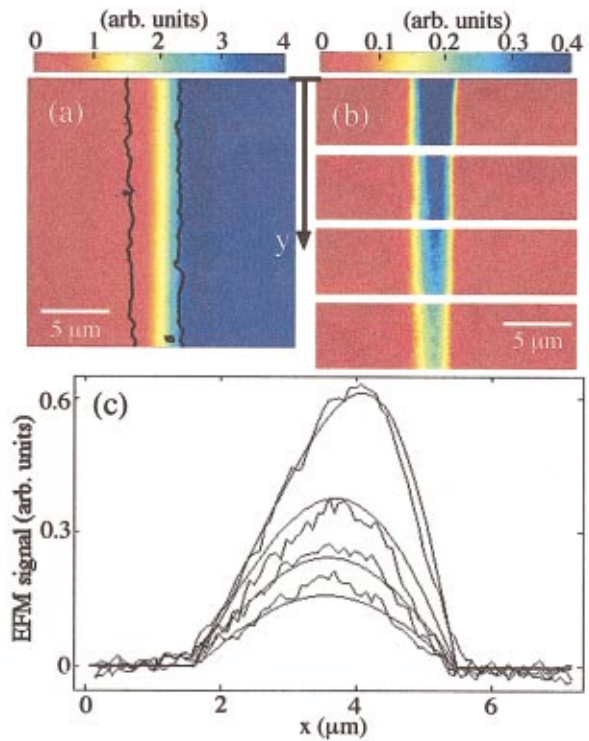


FIG. 4. (Color) EFM images for a device with long parallel electrodes. (a) Charging of the film, 48 min after $V_{dc} = -40$ V is turned on. The topographic contours of the electrodes are shown. (b) Slices of EFM images ($0 < y < 5 \mu\text{m}$) showing discharging of the film 0, 3, 6, and 9 min after V_{dc} is turned off. (c) Measured and calculated EFM signal plotted along the x axis.

the first image. As expected, the grounded drain electrode cannot be seen in the EFM image. The EFM signal changes in time and the charged region around the source grows as the charge spreads into the film [Fig. 2(a)]. Similar measurements on identical devices without depositing a film show no growth of the charged region at the electrode, guaranteeing that the charge motion is a property of the film.

Figure 2(b) shows the time evolution of the EFM images as the film discharges after the voltage on the source is set back to zero. Before the first line scan, the film has been charged for ≈ 60 min at $V_{dc} = -40$ V. Note that the voltage has been set to zero shortly after the scan has begun. The second scan is initiated 9 min after the first image. We have imaged samples charged for up to ~ 4 hr, required for the charge to reach the drain, and discharged over approximately the same time period. The completely discharged image looks equivalent to the image before charging.

During charging, the strong electric force near the source electrode influences the topographic contour making it impossible to measure the force at constant height. However, the force during discharging is much smaller, and we believe that discharging images directly give the square of the charge distribution in the film.

Figure 3 shows a series of line scans along the x axis for a constant y , corresponding to Fig. 2(b). The data are symmetrical around the center of the electrodes, and Fig. 3 shows the data on one side of the electrode; the edge of the electrode is set to $x = 0$. We show the line scan at $y = 0.3 \mu\text{m}$, close to the top of the images in Fig. 2(b). Line scans are

shown for times $t_1=0.05$ min, and $t_j=t_1+3(j-1)$ [min], $j=1,4,\dots,19$. The voltage on the source is set to zero at $t=0$. The narrow peaks in the EFM signal come from the roughness in the topography.

The calculated curves $[Q(x,t_j)]^2$ are obtained by fitting a diffusion model simultaneously to all the measured curves for $j=1$ to 21. We have used the analytical solution of a one-dimensional (1D) diffusion equation along x , applicable for line scans corresponding to positions far from the tip of the electrode. We first calculate the diffusion of charge from the electrode into the film: $Q_{\text{ch}}(x,t)=Q_0\{1-\text{Erf}(x/(2\sqrt{Dt}))\}$, for $x\geq 0$ and $t\geq 0$, where $\text{Erf}(\alpha)=2/\sqrt{\pi}\int_0^\alpha e^{-s^2}ds$, and D is the diffusion coefficient. This solution satisfies $Q(x,t)=Q_0$ for $x=0$, $t\geq 0$, and $\lim_{x\rightarrow\infty}Q(x,t)=0$. The charge distribution during discharging is $Q_{\text{disch}}(x,t)=Q_{\text{ch}}(x,t+\tau_{\text{ch}})-Q_{\text{ch}}(x,t)$, where $x\geq 0$, $t\geq 0$, and τ_{ch} is the charging time. We assume $Q_{\text{disch}}(x,t=0)=Q_{\text{ch}}(x,\tau_{\text{ch}})$, and $Q_{\text{disch}}(x=0,t)=0$ at all times. The fit parameters are Q_0 and D , although Q_0 is no longer a parameter when the data are normalized. It is also necessary to allow the duration of charging τ_{ch} and the time t_1 of the first line scan to vary, as discussed later. For subsequent scans, we use $t_j=t_1+3(j-1)$ [min], for $j=1$ to 21.

Good agreement between calculated and measured curves is obtained. Figure 3 shows every third curve $j=1,4,\dots,19$. From the best fit $D=(2.8\pm 0.2)\times 10^{-3}$ $\mu\text{m}^2/\text{s}$, $\tau_{\text{ch}}\approx 340$ min, and $t_1=0.35$ min. The value of D is robust to the variation of other fit parameters. The actual measured values $\tau_{\text{ch}}=60$ min and $t_1=0.05$ min are much shorter than the best-fit values. Allowing τ_{ch} and t_1 to be larger than measured has the effect of broadening the initial charge distribution. This may be compensating for our finite spatial resolution, not included in the model. For $j\geq 2$, the difference in t_1 is insignificant.

The same NC film was also imaged during illumination with green laser light (with energy above the CdSe NC band-gap). From the fits to the discharging data in this case, $D=(4.9\pm 0.2)\times 10^{-3}$ $\mu\text{m}^2/\text{s}$.

As argued earlier, the charging data in Fig. 2(a) are not recorded at a constant height. Specifically, the applied voltage V_{dc} causes the source to appear larger than for $V_{\text{dc}}=0$; the apparent increase ~ 1.4 times of the electrode height implies that the height at which the EFM signal is recorded varies from 200 to 245 nm across the scan. From the measured z -dependence $\Delta\phi(x,y)\propto V_{\text{dc}}^2/z^{1.3}$, we infer that the EFM signal above the electrode is $\sim 80\%$ of the value expected for a specified height of 200 nm.

Figure 4 shows the EFM images, under the same conditions as for Fig. 2, for a device with 800- μm -long parallel electrodes, separated by ~ 4 μm . The NC diameters are ≈ 4.7 nm.⁹ Figure 4(a) shows the EFM image after charging of the

film for 48 min, while Fig. 4(b) shows the discharging of the film, previously charged for ≈ 2 h. The four images are slices ($0<y<5$ μm) of EFM scans which are begun 0, 3, 6, and 9 min after V_{dc} is turned off. Figure 4(c) shows the measured and calculated EFM signal plotted along the x axis for $y=4$ μm from the top of the scan, during the discharging. Line scans are shown for $t_1=0.33$ min, $t_j=t_1+3(j-1)$ [min], for $j=1$ to 4. The calculated curves are from a 1D diffusion and we use $t_1=1.8$ min, larger than the actual value as for Fig. 3. We find $D=3.6\times 10^{-3}$ $\mu\text{m}^2/\text{s}$ for the film.

The resistance per square of the film $R=1/DC$, where C is the capacitance per unit area. The capacitance $C=\epsilon_0\epsilon_r/h\approx 10^{-16}$ F/ μm^2 , where $\epsilon_r\approx 4$ for SiO₂, and $h=350$ nm is the thickness of the SiO₂ layer. For $D=3\times 10^{-3}$ $\mu\text{m}^2/\text{s}$, $R\approx 3\times 10^{18}$ Ω/square . Even for the geometry in Fig. 2, this corresponds to $R\sim 10^{16}$ Ω and a steady-state current $I\sim 10^{-15}$ A at -40 V. This could not have been detected in previous experiments.⁶ We estimate that this technique could be used to measure resistances per square as high as $\sim 10^{20}$ Ω using thicker oxides.

In conclusion, we have imaged the charge transport in films of CdSe NCs, and have measured the diffusion coefficient directly. Future measurements of the charge diffusion as a function of temperature will tell us whether the diffusion model continues to describe the transport at low temperatures. This method can be applied to systems with currents so small that they cannot be measured by conventional methods. It will also allow quantitative studies of anomalous diffusion, which may result from electron interactions. Higher spatial and temporal resolution can be achieved using thinner oxides and small sample areas, respectively.

We thank D. Novikov and L. Levitov for helpful discussions. This work was supported by the NSF under MRSEC (DMR 02-13282) and under NSEC (PHY-0117795).

¹For a review, see *Scanning Probe Microscopy and Spectroscopy, Theory, Techniques and Applications*, edited by B. Bonnell (Wiley-VCH, New York, 2000).

²M. Bockrath, N. Markovic, A. Shepard, M. Tinkham, L. Gurevich, L. P. Kouwenhoven, M. W. Wu, and L. L. Sohn, *Nano Lett.* **2**, 187 (2002).

³A. Bachtold, M. S. Fuhrer, S. Plyasunov, M. Forero, E. H. Anderson, A. Zettl, and P. L. McEuen, *Phys. Rev. Lett.* **84**, 6082 (2000).

⁴E. Tevaarwerk, P. Rugheimer, I. M. Castellini, D. G. Keppel, S. T. Utley, D. E. Savage, M. G. Lagally, and M. A. Eriksson, *Appl. Phys. Lett.* **80**, 4626 (2002).

⁵T. D. Krauss and L. E. Brus, *Phys. Rev. Lett.* **83**, 4840 (1999); T. D. Krauss, S. O'Brien, and L. E. Brus, *J. Phys. Chem. B* **105**, 1725 (2001).

⁶N. Y. Morgan, C. A. Leatherdale, M. Drndić, M. V. Jarosz, M. A. Kastner, and M. G. Bawendi, *Phys. Rev. B* **66**, 075339 (2002).

⁷D. S. Ginger and N. C. Greenham, *J. Appl. Phys.* **87**, 1361 (2000).

⁸C. B. Murray, C. R. Kagan, and M. G. Bawendi, *Annu. Rev. Mater. Sci.* **30**, 545 (2000); C. B. Murray, D. J. Norris, and M. G. Bawendi, *J. Am. Chem. Soc.* **115**, 8706 (1993).

⁹M. G. Bawendi and N. E. Scott, US Patent Application 20,020,071,952, 2002.